Storm Wave Resonance Controlled by Hollow Block Structures

by

F. Büsching[1]

ABSTRACT

The formation of long shore bars in front of sandy beaches often is assumed to act as a shore protecting feature only. At Sylt Island/Germany, however, boundary conditions formed by a structured long shore bar, running roughly parallel to the shoreline, are found to be the reason for intense *resonance absorption effects* at storm surge conditions as well. Incoming waves interact with the water level deflections in the trough located between the bar and the beach in such a way that frequency components match a limited number of possible harmonics of the enclosed body of water. As there are significant energy densities to be found in the wave energy spectra at harmonic numbers 1 through 5 of the enclosed water body, this phenomenon is believed to be responsible for the tremendous coastal recessions at this island due to storm surge occurrences in the past.
The existence of resonant seiching modes is deduced from intense low frequency *anomalous dispersion effects* (ADE), which had been found previously.
Wave tank investigations also demonstrating the *combined effect of resonance and anomalous dispersion* are reported in detail. Based thereon the former field investigations, executed on Sylt Island, are analysed again. As a consequence of the kind of resonances found, extreme water level deflections are expected to occur not only at the beach face but also at the landward slope of the long shore bar. That is why a special type of protective structure, consisting of hollow concrete blocks, is suggested to be placed on top of the ridge.

1. INTRODUCTION

Seiching is described as the formation of standing waves in water body, due to wave formation and subsequent reflections from the ends. It is well known that these waves may be incited in enclosed bays or harbours by earthquake motions or impulsive winds over the surface. In case that periodical wave motions entering a basin are considered also, boundary conditions of resonance are given, because the system is exited by the continued application of external forces at a natural frequency. In general the phenomenon of resonance is widely known in various fields of physics. Especially, however, from electromagnetic wave propagation in dielectrics it is recognized that resonant absorption is accompanied by an anomalous dispersion effect.
As a result from field measurements on storm surge waves at the west coast of Sylt Island / Germany the author formerly had observed such phenomena of intense *anomalous dispersion effects* (ADE: $dc/df > 0$, BÜSCHING (1978)), which had been unknown before with respect to shoaling and breaking gravity waves. (The classical dispersion relation merely describes a normal dispersion $dc/df \leq 0$, with the limiting value $dc/df = 0$ at shallow water.) Hence, later on the author searched for an explanation just referring to analogues of resonance absorption of electromagnetic waves, BÜSCHING (1982, 1983). In this context also the interaction of partly standing waves with the washing movement of broken waves on a steep slope should be mentioned, BÜSCHING (1991 – 1999).
In the last years an ADE, however, had impressively been verified by model investigations at Bielefeld University of Applied Sciences (BUAS), relating to resonance phenomena occurring in a wave tank. Therefore the author considers the boundary conditions at Sylt Island - formed by a long shore bar in front of a sloping beach - also to act as a basin, in which the water body is in resonance with waves coming from sea especially at storm surge conditions.
In the following the results of the above tank investigations are reported in detail. Based thereon in turn the former field investigations, executed on Sylt Island, are analysed again. As the ADE actually documents the thesis of a prominent phenomenon of resonance, such a result may be pretty relevant with respect to the understanding of energy dissipation processes in the near shore zone.
In particular, because the shape of any harmonic is assigned by maximum water level deflections (loops superimposing to produce breakers) at the beach and at the landward slope of the long shore

[1]Prof. Dr.-Ing., Bielefeld University of Applied Sciences, Diesselhorststr.01, D-38116 Braunschweig, Germany, Fax: +49 (0)531 2512008, buesching@hollow-cubes.de

bar, influencing (reducing) merely the movements at the bar will reduce the breaking action at the beach as well.

2. MODEL INVESTIGATIONS IN THE WAVE TANK OF BIELEFELD UNIVERSITY OF APPLIED SCIENCES (BUAS)

A rather big number of model investigations (scale 1:5) had been executed in the wave tank of BUAS in order to demonstrate the efficiency of so-called “Hollow Block Revetment Structures” patented in 1991, see BÜSCHING (1991-1999). Such structural elements are assigned by much less destroying energy affecting a sloping dam structure compared to a conservative design. This is brought about

- by a modified coupling between partial standing waves in front of the sloping structure and the washing movement on the slope face (damped resonance, see above) and
- by rough turbulent influx and efflux from the revetment structure.

For further details refer to BÜSCHING (2001). Moreover a proposal for a structure modifying boundary conditions of the ridge (chapter 6 of this publication) is based on the respective patent.
With respect to the topic of resonance absorption, however, the method of measurement is important only, which was adopted equally for the judgment of reflection effects at the hollow block revetment as well as at the smooth referential slope. The actual evaluations, however, refer to the boundary conditions of the smooth referential slope inclined 1:m = 1:3 only, see Fig.08. At the wave generator an input spectrum was used, which - scaled up to prototype - resembled those measured at the beach stations on Sylt Island, confer BÜSCHING (1975, 1976).
Hence, substantial energy densities in the model input spectrum are concentrated in the frequency range $0.48\ \text{Hz} \leq f \leq 0.62\ \text{Hz}$.
In the present case no precautions had been made in order to prevent re-reflection from the wave maker. One has to point out that such a procedure normally will not by applied for wave tank investigations, because the re-reflection phenomenon usually will not be expected in a natural environment. Moreover - deviating from familiar methods - the tests had been carried out comprising a rather big number of 90 wave probe stations equally spaced 10 cm in the perpendicular line in front of the slope. The signals from the wave probes were recorded quasi synchronously and were processed by spectrum analyses confined to a total frequency range $0.03263 \leq f \leq 1.3997\ \text{Hz}$.

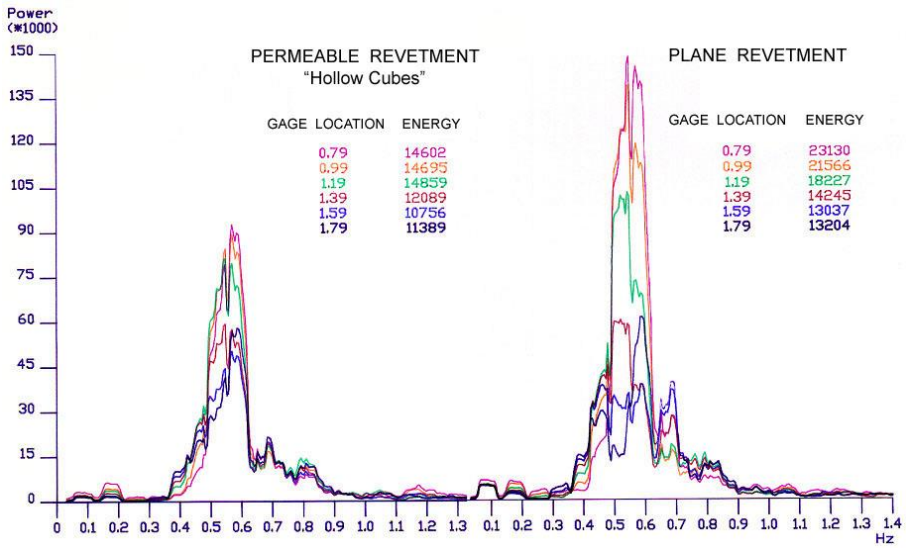

Figure 01: Synchronously Measured Energy Spectra (of water level deflections) in Front of a Permeable Revetment Structure and a Plane Revetment Structure of Slope 1:3.

Hence, statements could be made

- on the energy content of subdivided frequency bands and
- on the associated reflection coefficients depending on frequency $C_R(f)$, see BÜSCHING (1992).

The calculated energy spectra represent a special kind of composite energy spectra, because there are water level deflections of incoming waves, reflected waves and re-reflected waves superimposing at any gage station. As an example in Fig.01 there are plots of spectra synchronously taken at 6

different gage locations in front of the permeable (hollow) slope and in front of the smooth plane slope respectively. In particular the spectra demonstrate the changes of energy content along the slope in the area extending from the structure toe (station 1.79m) to the zone of maximum breaker instability (stations 1.19m to 0.79m).
In the following 3 diagrams (Fig.02 – Fig.04) values of the integrated spectrum area IA (variance) are plotted along with the gage station distance from the slope face, i.e., from the point IP of the still water level (SWL) intersecting the slope, which is also sketched in relation to the probe stations at the bottom of Fig.02.

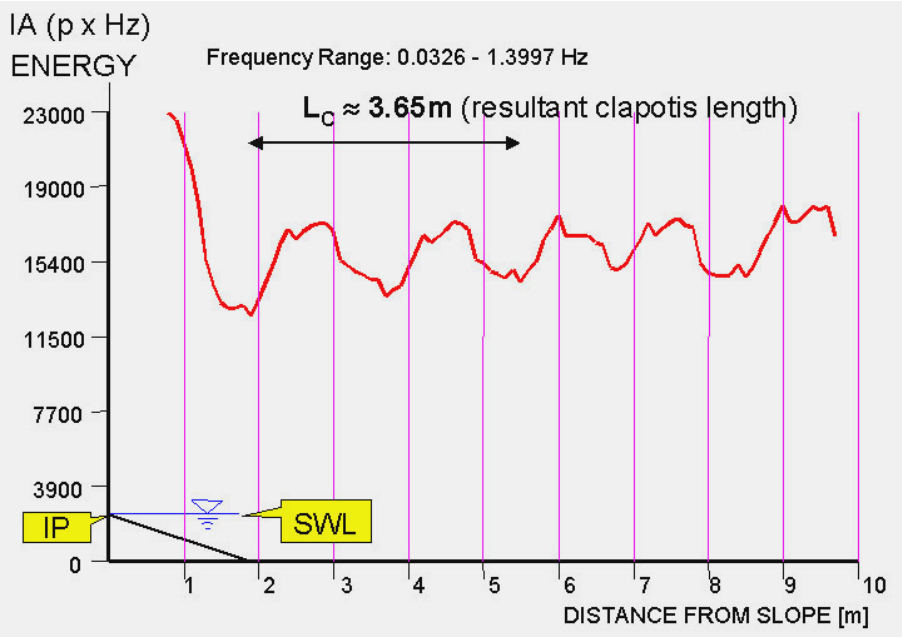

Figure 02: Integral Values of Spectral Energy of the Total Frequency Range 0.03 ≤ f ≤ 1.4 Hz Documenting the Existence of a Partial Clapotis in Front of the Slope 1:m = 1:3.

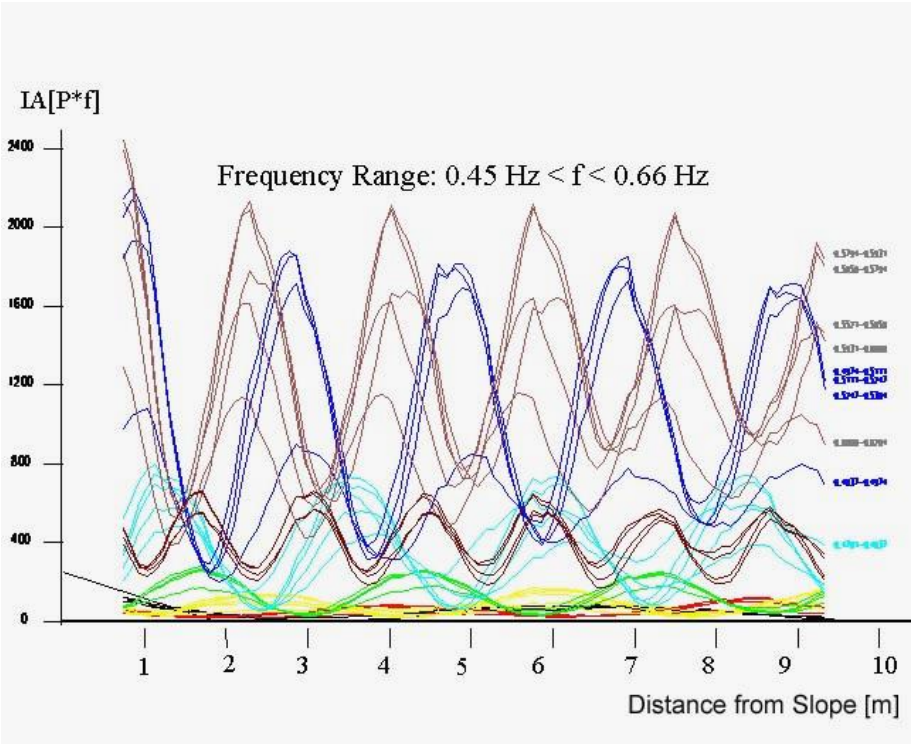

Figure 03: Energy Enclosed in Enlarged Energy Containing Frequency Intervals $n \cdot \Delta f$ of the Frequency Range 0.45Hz ≤ f ≤ 0.66 Hz.

Because the variance is proportional to the wave energy (of vertical water level deflections) contained

in the respective frequency range, changes in those plots can be interpreted with respect to the actual position and dominance of the partial clapotis in relation to the sloping structure.
In Fig.02 the variation in the plot of the total energy indicates that the length of a “resultant Clapotis” is about L_C = 3.65m (distance between the first and third minimum of energy). Although there are some disturbances to be seen in the plot, it will be shown that conclusions of good quality can be drawn from that data, provided that the total frequency range is subdivided into a number of smaller frequency ranges and noise frequency ranges are disregarded.
Because of insufficient graphic resolution, a respective representation of all 256 frequency components (spaced Δf = 0.00543 Hz) separately was abandoned.
The essential phenomenon, however, comes out clearly enough from Fig.03, where lines of energy relating to enlarged frequency intervals ($n \cdot \Delta f$) are calculated for a confined frequency range 0.45Hz ≤ f ≤ 0.66 Hz. It can be seen clearly that there are lines of energy, possessing similar energy distributions in the length expansion, relating to the distance from the sloping structure (point IP); i.e., they have same distances between neighboring energy minima or neighboring energy maxima respectively and same phase angles.
The wave measurements had been executed by BLEES and STÜHMEYER (1991) while the respective calculations aiming at data reduction had been performed by HAGEMEYER and KRAMER (1992).
As a result 82 discrete energy lines were found, which could be assigned to 12 definable sub-ranges within the frequency range 0.4015Hz ≤ f ≤ 0.8030 Hz, see Fig.04.

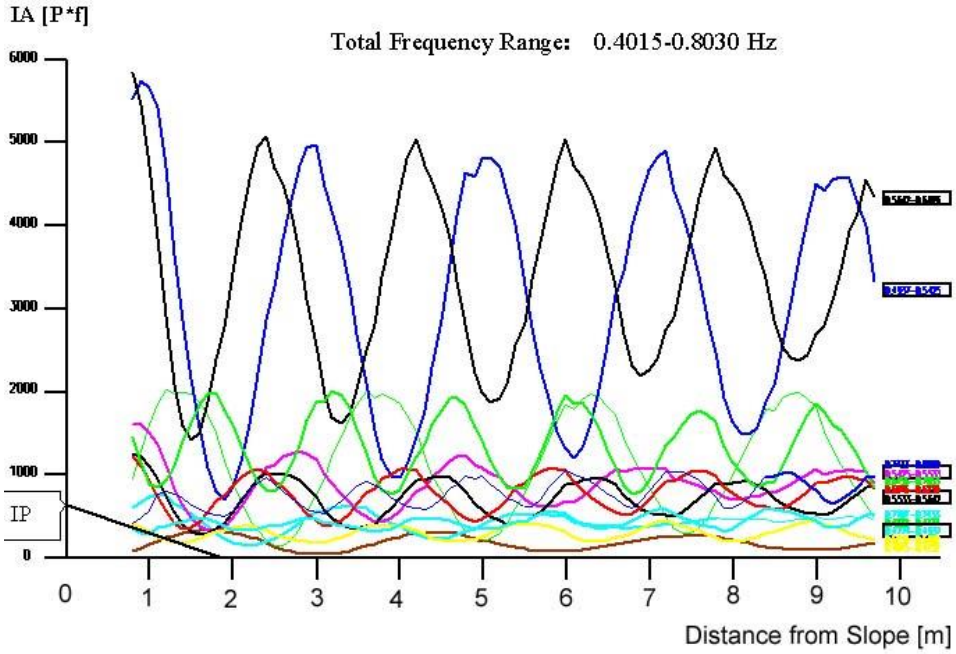

Figure 04: Energy Content of 12 Definable Partial Standing Waves (→ Partial Waves)

Thus the partial clapotis, documented in Fig.02, can be recognized approximately as the resulting wave from 12 superimposing partial clapotis waves existing coincidentally in the wave tank.
In order to distinguish the resultant partial clapotis from its components in the following the latter shall be named shortly “partial waves”.
The general properties of partial clapotis waves or partial waves respectively can be derived from their energy distribution in the length expansion as shown in Fig.05. Particle movements at phases of clapotis loops can be approximated by ellipses possessing bigger vertical principle axis and those at phases of nodes by ellipses possessing bigger horizontal principle axis. The varying reflection effects with distance from the slope may be described by shortening principle axis while minor axis increase.
Additional information on resulting wave deformation are contained in BÜSCHING (2000, 2001) and evaluations relating to reflection coefficients depending on frequency can be found in BÜSCHING (1992). The most striking outcome, however, with respect to the above data analysis, is the fact that partial waves – disposing of equal component lengths - must obey an anomalous dispersion law dc/df > 0: At a given water depth phase velocity $c = L \cdot f$ increases with frequency.

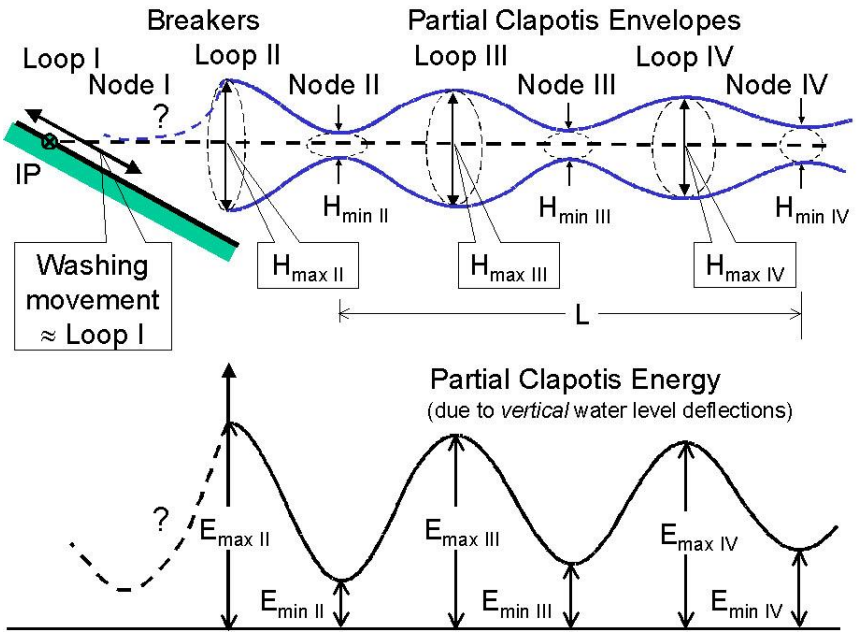

Figure 05: Sketch of Partial Standing Waves at a Slope.
Upper Part: Partial Clapotis Envelopes
Lower Part: Partial Clapotis Energy

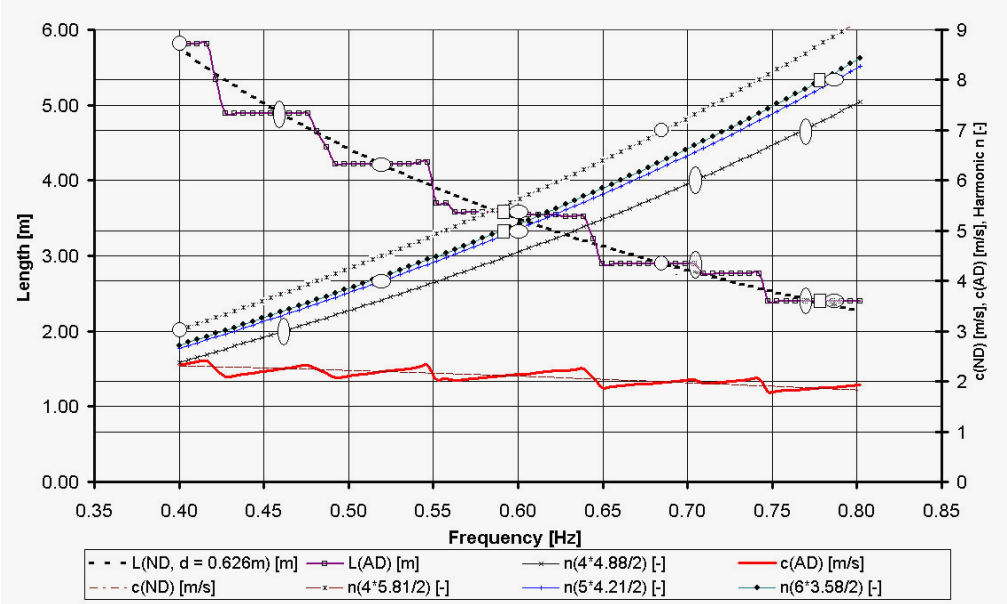

Figure 06: Component Lengths L, Phase Velocities c and Harmonic Numbers n Plotted with Frequency.

In the upper part of Fig.06 the lengths associated with the 82 energy lines, mentioned above, are denoted L(AD)(f) (AD = anomalous dispersion), whereas L(ND)(f) (ND = normal dispersion; dashed line) refers to the classical dispersion relation according to water depth d = 0.626 m in the wave tank. Both curves can be named “Length Spectra”.
The corresponding plots of phase velocities c(AD)(f) und c(ND)(f) (Phase Velocity Spectra) are shown in the lower part of the figure.
Because of the stepped structure of L(AD)(f) suggesting the existence of different oscillatory modes of the enclosed water body in the tank coincidentally, in the following it will be shown that boundary conditions are compatible with higher harmonics.
It is well known that natural frequencies of a water volume in a basin disposing of vertical walls can be calculated in using formula (01):

$$f[Hz] = (n+1) \cdot \frac{c}{2 \cdot D} \qquad (01)$$

where
D = horizontal wall distance,
c = wave celerity and
n = harmonic number.

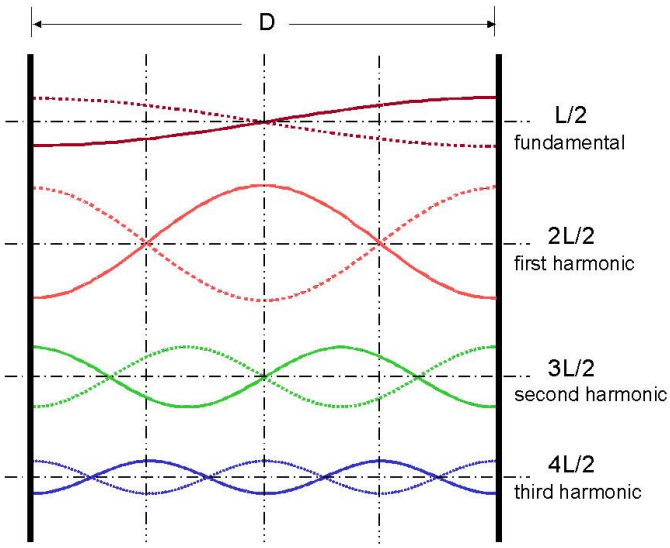

Figure 07: First 4 Theoretical Oscillatory Modes of a Water Body in a Basin Disposing of Vertical Walls at Distance D

n = 0 denotes the fundamental oscillation and n = 1, 2, 3...are named first, second, third harmonic etc., Fig.07. Solving formula (01) with respect to harmonic numbers n[-], yields formula (02)

$$n(f)[-] = \frac{2 \cdot D \cdot f}{c} - 1 \qquad (02)$$

Applying $c = L \cdot f$ yields formula (03)

$$n(L)[-] = \frac{2 \cdot D}{L} - 1 \qquad (03)$$

At boundary conditions consisting of a slope at one side and a moving flap at the other (Fig.08) no distinct distance D can be suggested.
That is why multiples of half-wave length of the 4 dominating longest partial waves (5.81m, 4.88m, 4.21m und 3.58m) were used together with the theoretical phase velocity, see Fig.08.

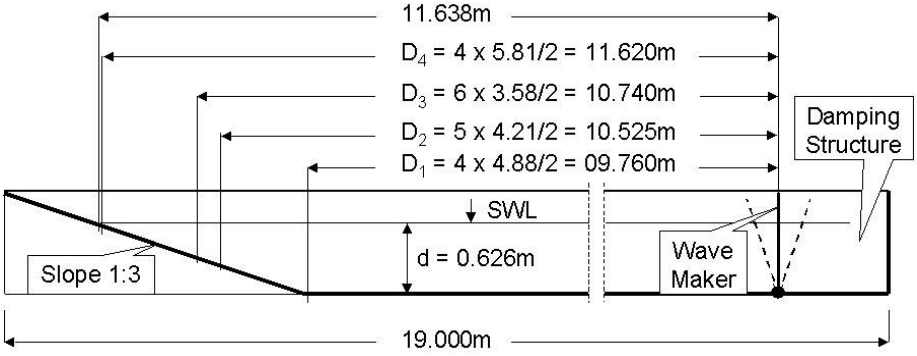

Figure 08: Different Distances D_i with Respect to the Hinge of the Flap (schematically, without scale)

Defining the minimum distance between wave maker and the toe of the slope by
D_1 = 4 x 4.88/2 m = 9.76m, confer Fig.08,
then distances
D_2 = 5 x 4.21/2 = 10.525m,
D_3 = 6 x 3.58/2 = 10.74m and
D_4 = 4 x 5.81/2 = 11.62m
mark different points on the wet slope.
Hence, according to such 4 distances there are also 4 different functions $n_i(f)$ in Fig.06. It can be seen clearly that the partial waves represent higher harmonic numbers $3 \leq n \leq 8$.
The fact that several harmonics obviously are linked by the same fundamental oscillation, actually confirms the existence of oscillatory modes pronounced by resonance.
Thus intrinsic *resonance frequency ranges* are defined by frequency components disposing of nearly equal wave lengths. With respect to the function c(AD)(f) deviating distinctly from c(ND)(f) (Fig.06), the resonant components can be identified by the steps in the phase velocity function. Portions of anomalous dispersion ($dc/df > 0$) are neighbored by portions of *stronger* normal dispersion ($dc/df << 0$). It is interesting that such a characteristic indeed resembles resonance features well known from electromagnetic waves propagating through dielectrics.
In order to link dispersion characteristics additionally to the energy content of the partial waves, the functions of Fig.06 are to be seen in Fig.09 also, however transformed to the wave lengths axis.
(Note that the horizontal axis is shown side-inverted in order to ease comparison with Fig.06.)
Referring to c(AD)(L), it is even more impressive, that the respective deviation is documented by jumps. Here there is $dc/dL << 0$ tending to the limiting value $dc/dL \rightarrow \pm \infty$, while in the wave lengths ranges between the discrete spots of resonance there are stronger gradients $dc/dL > 0$.

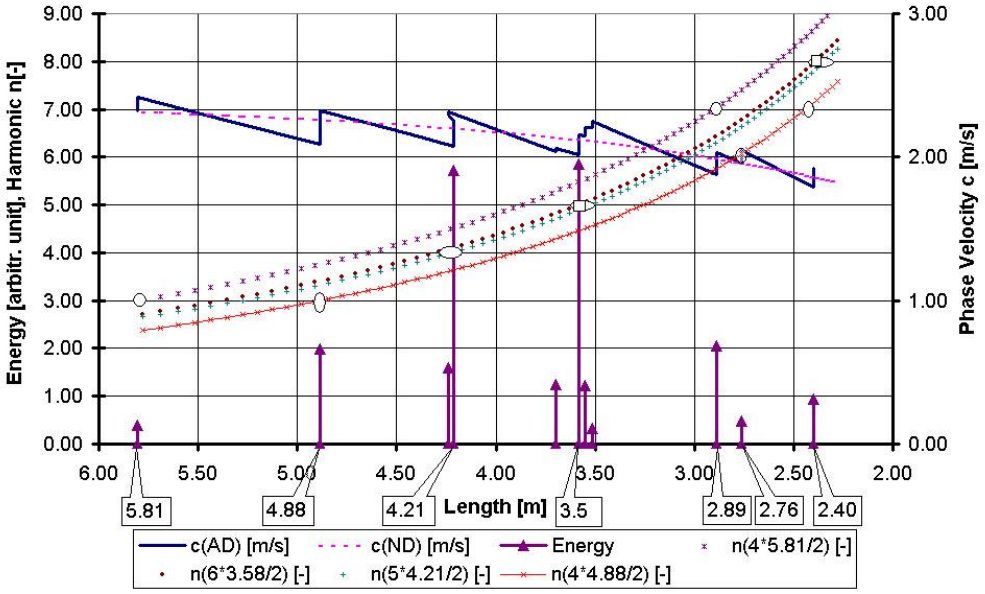

Figure 09: Phase Velocities c, Harmonic Numbers n_i and Energy Plotted with Lengths of Partial Waves

Additionally the values of energy are allotted to the respective lengths of partial waves. It can be seen that maximum energies of nearly equal amount belong to partial wave lengths 4.21m and 3.58m.
Calculating the arithmetic mean wave length from all partial waves (weighted with the energy) obviously such a wave length corresponds to the resultant partial clapotis length L_C = 3.65m found from Fig.02.
At last the 4 functions of oscillatory mode numbers also are plotted as $n_i(L)$ within Fig.09.

3. STORM WAVE RESONANCES AT WESTERN COAST OF SYLT ISLAND.

Water level deflections $\eta_{100}(t)$ and $\eta_{85}(t)$ synchronously measured at two locations on the beach (to be seen from Fig.10) repeatedly had been the matter of previous analyses carried out by the author. Information not directly necessary for the understanding of the actual topic will not be repeated here and can be found in the references.

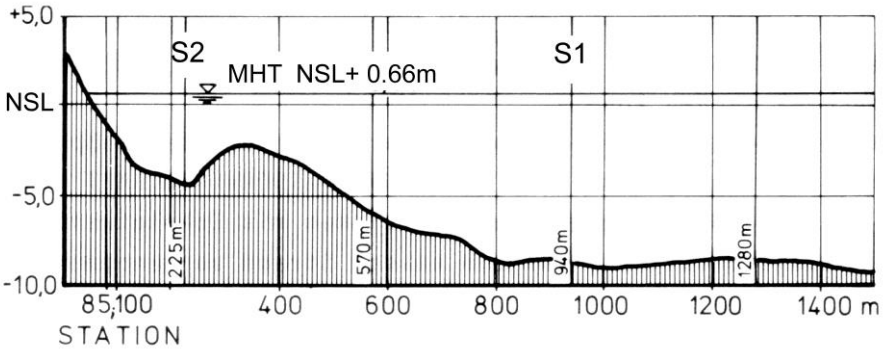

Figure 10: Gage Location at Westerland/Sylt, 1973. Near Shore Stations S1: 940m, S2: 225m; Beach Stations 100m and 85m

The total measuring campaign extended from December 13, 12.30 to December 14, 1973, 18.38. The following spectral functions (according to record length T_R = 819.2 s) were calculated at 16 intervals distributed over the 30 hours period irregularly, BÜSCHING (1974):

Energy spectra $G_{xx}(f)$ and $G_{yy}(f)$ with reference to stations at x = 100m and at y = 085m,

Transfer functions $H_{xy}(f)$ cut into magnitude $\overline{|H_{xy}|}(f)$ and phase $\varphi_{xy}(f)$ and

Coherence functions $\overline{\gamma}^{2}_{xy}(f)$.

Based on the phase information $\varphi_{xy}(f)$ (of the transfer function) previously the spectrum of phase velocity had been defined as follows (BÜSCHING (1978):

$$c(f) = \frac{\overline{xy}}{\varphi_{xy}(f)/2 \cdot \pi \cdot f} \qquad (04)$$

where

$\overline{xy}$ = the distance between stations x and y (=15m) in the coast normal control line and $\varphi_{xy}(f)$ = the phase difference between the Fourier components of frequencies f_i at those stations.

Because of the fact that the special phenomenon of anomalous dispersion in the above model investigations could be deduced from the distinct deviations in the length spectrum of partial waves, henceforth in the following such kind of a spectrum also will be analyzed here with reference to the field investigations.

This can be deduced from the anomalous phase velocity spectrum ($dc/df > 0$) as follows:

$$c(f) = L \cdot f = \frac{\overline{xy}}{\varphi_{xy}(f)/2 \cdot \pi \cdot f}$$

$$L(f) = \frac{\overline{xy}}{\varphi_{xy}(f)/2 \cdot \pi} \qquad (05)$$

Of course a comparison between the results of the above model investigations and the field measurements is reasonable only, if sufficient geometric and hydraulic similarity of the wave kinematics is given.

As data analysis referring to the model was restricted to the kinematics of partial reflected waves, for the time being measuring periods of maximum tide water levels during field investigations are considered exclusively. Doing so, it is guaranteed that partial reflection is dominating the mechanisms of wave breaking or even of the washing movement of broken waves. At the same time the analysis is confined to those measurements disposing of sufficient coherence values of about $\overline{\gamma}^{2}_{xy} \approx 0.8$.

For better comparison all the spectral functions of measurement number 11 (December 14, 1973, 03.46, water depth d = 4.5m) are placed one beneath another in Fig.11 through 13.

Because of space limitations, only two out of four additional similar measurements at water depths d ≥ 3.6m can be shown here in the appendices, chapter 7.

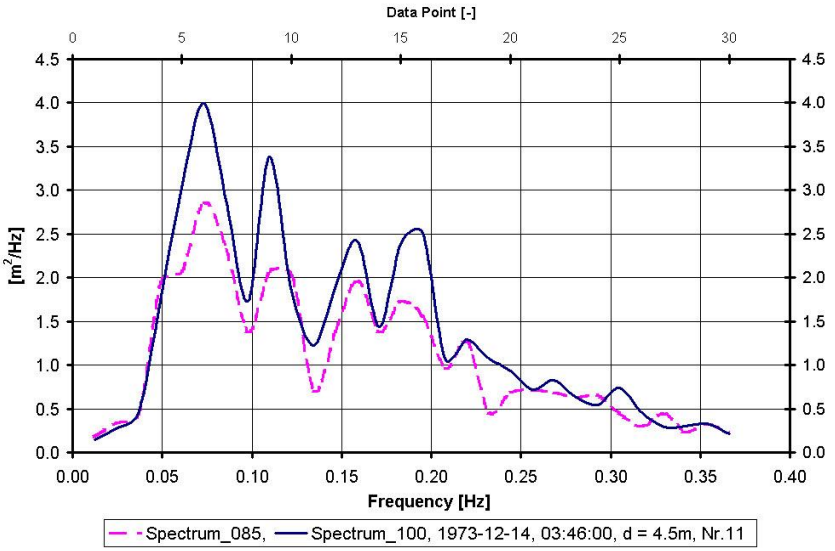

Figure 11: Synchronously Measured Energy Spectra of Storm Waves at Stations 100m and 85m (see measuring profile of Fig.10)

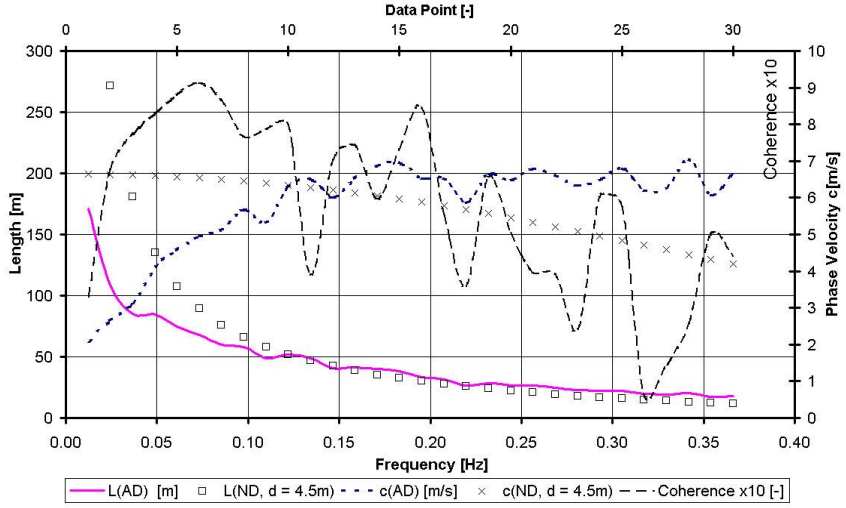

Figure 12: Spectra of Phase Velocities c(f), Lengths L(f) and Coherence (tenfold values)

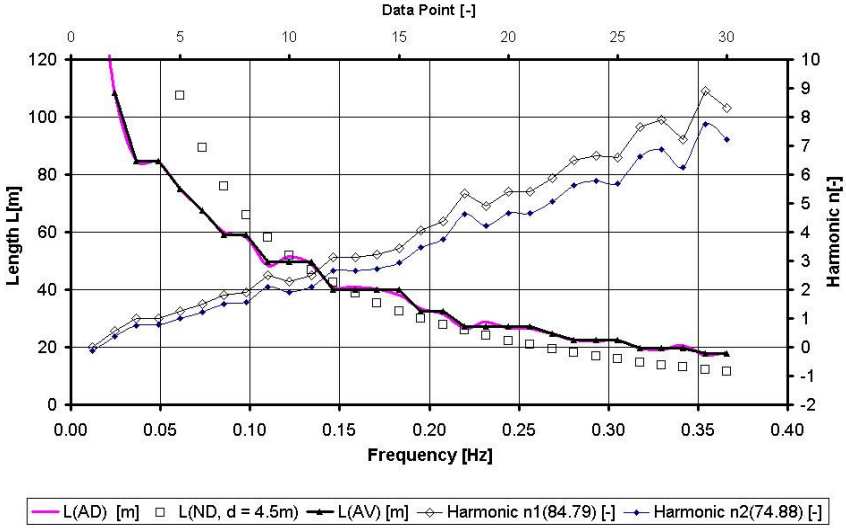

Figure 13: Enlarged Lengths Spectrum L(f) and Harmonic Numbers $n_i(f)$

In Fig.11 the two energy spectra are characterized by maximum energy densities and significant wave heights respectively:

$\max E_{fp,100} = 3.99 m^2/Hz$ resp $H_{S,100} = H_{m0,100} = 2.91 m$ and

$\max E_{fp,085} = 2.85 m^2/Hz$ resp $H_{S,085} = H_{m0,085} = 2.59 m$.

Because of the energy decreasing from station 100m to station 85m (nearly equally at the energy containing frequencies), no resonance phenomena can be recognized at least due to the washing mechanisms.

In Fig.12 there are plotted the classical dispersion relation as well as the spectra of the phase velocity c(f) and of the wave length L(f) both based on the phase information of the transfer function. Additionally the coherence function $\overline{\gamma}^{-2}_{xy}(f)$ (tenfold values) is shown.

It shall be pointed out here that the coherence values in the frequency range $0.03 Hz \le f \le 0.2 Hz$ are surprisingly high, although at the particular measuring time gust wind speeds of U > 33m/s (BFT 12) had been measured. That circumstance after all had been the reason, why the author previously allotted high confidence to the phenomenon of intense anomalous dispersion in that portion of the phase velocity spectrum c(AD)(f), which cannot be explained by nonlinear effects only.

By contrast to the classical dispersion relation c(ND)(f), describing normal dispersion $dc/df \le 0$, anomalous dispersion just disposes of the opposite sign.

Regarding the wave length spectrum L(ND)(f), calculated in using the classical dispersion relation, it can be stated that there is an absurd increase of wave lengths with the frequency approaching zero. This statement remains true also in the case that smaller water depths are used in the respective formula, see appendices 01a and 02a.

Contrary, however, the values of the anomalous wave length spectrum L(AD)(f) match the real measured wave lengths satisfyingly, conf. FÜHRBÖTER (1974) and BÜSCHING (1978, 1979).

In order to perform an advanced analysis of the wave length spectrum L(AD)(f) enlarged plots of both length spectra are contained in Fig.13.

Comparing Fig.13 with Fig.12 it can be seen clearly that the stepped structure of the length spectrum L(AD)(f) is due to the distinct deviations (dc/df >0) in the corresponding phase velocity spectrum c(AD)(f) (Fig.12). Additionally the function L(AV)(f) is plotted, by which average wave lengths are given - related to some neighboring frequency points.

Hence, there is a result similar to that one of the model investigations.

Reliability of such a result is proven by the fact that the 4 additional measurements also show the phenomenon, see appendices 1a and 2a. Moreover it can be found also in all remaining storm surge measurements, executed at smaller water depths and at less wave intensities.

At last - according to formula (02) - there are two functions describing the harmonic numbers n(f) contained in Fig.13.

Calculating n1(f) the mean value L(AV) = 84.79m (near f = 0.045 Hz) was supposed to represent a first harmonic. In this case the second harmonic can be found near f = 0.09 Hz and the third harmonic approximately at f = 0.17 Hz etc.

Because the phase velocity depends on frequency, it is clear that frequencies of higher harmonics do not match exactly the whole-numbered multiples of the fundamental oscillation. This also holds, if L_P = 74.88 m (near the spectral peak at f = 0.06 Hz) is supposed to represent a first harmonic accompanied by a second harmonic at f ≈ 0.12 Hz etc.

Although coherence at the first frequency point f = 0.012207 Hz seems to be insufficient ($0.3 \le \overline{\gamma}^{-2}_{xy} \le 0.4$) (Fig.12), there is some evidence that also the fundamental oscillation, disposing of a length of about 170m, exists in the trough between the ridge and the beach. In the wave lengths plots belonging to distinct single peak energy spectra (see appendices 1a and 2a) the fundamental oscillations can be recognized representing maximum wave lengths.

(In this context it can be mentioned here that a fundamental oscillation disposing of a node at the long shore bar (- supposing a semi-enclosed (open) basin -) would not offer proper harmonic numbers.)

Similar to Fig.09 (model investigations) the spectra of phase velocities c(ND)(f) and c(AD)(f) (Fig.12) had been transferred into spectra c(ND)(L) and c(AD)(L) respectively, confer curves in the upper part of Fig.14. c(AD)(L) is shown, however, confined to the frequency range $0.03 Hz \le f \le 0.18 Hz$ only, where mean coherence values are about $\overline{\gamma}^{-2}_{xy} = 0.8$. As expected in the spectrum c(AD)(L) jumps ($dc/dL \to \pm\infty$) also appear, by which the higher harmonics can be identified. The corresponding

harmonic numbers n1(L) and n2(L) are shown in the lower part of the figure. Contrary to the model investigations, however, only adjacent to the second and the third harmonic there are stronger

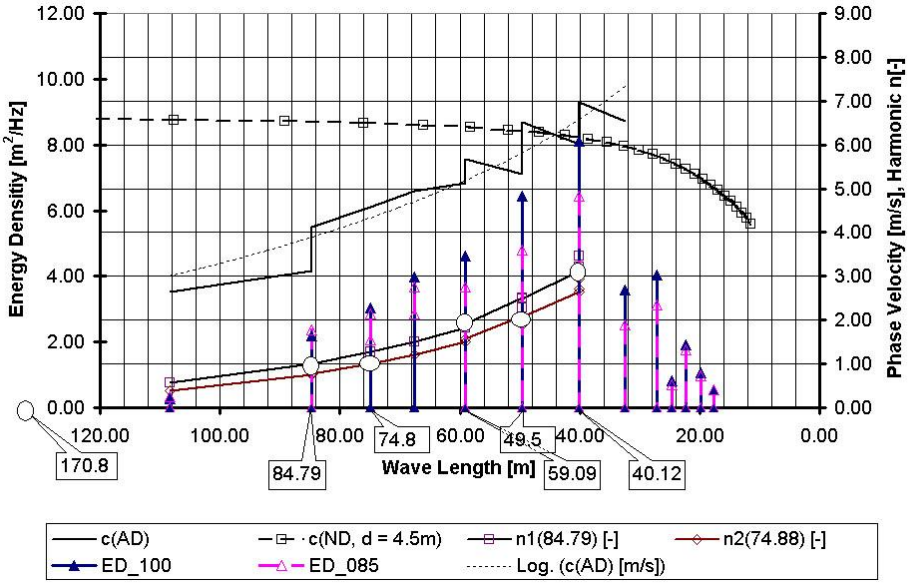

Figure 14: Phase Velocities c(ND)(L) and c(AD)(L), Harmonic Numbers n(L) and Line Spectra of Energy Density ED(L)

gradients dc/dL > 0 compared to that of c(ND, d = 4.5m), while the total trend is dc/dL < 0, representing anomalous dispersion.

Finally in Fig.14 and Fig.15 the line spectra of energy densities ED(L) are plotted with reference to stations 100m and 85m. Such values, related to discrete wave lengths, had been calculated by summing up the single amounts of energy densities of frequency components disposing of (nearly) equal wave lengths.

With reference to station 100m the maximum energy density max ED(L) = 8m²/Hz belongs to a wave length L(AD) = 40m.

By contrast in the frequency spectrum there is a maximum energy density of about maxEP(f) = 4m²/Hz and applying classical normal dispersion the corresponding wave length is LP(ND) ≈ 90m >> L(AD) ≈ 40m, see Fig.15.

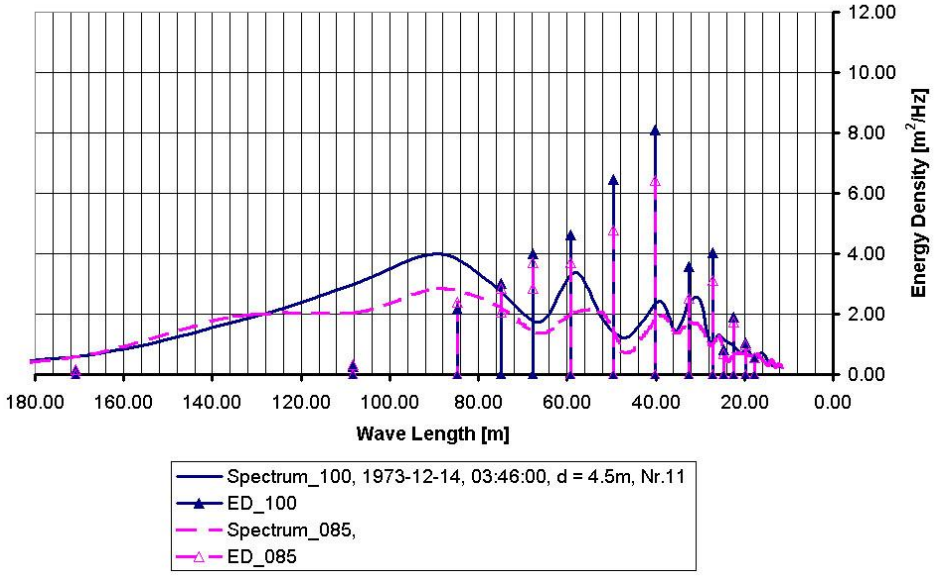

Figure 15: Energy Density Spectra Transferred to the Length Axis Applying Classical Dispersion Relation and Line Spectra of Energy Density ED(L) Calculated on the Basis of the Anomalous Length Spectrum L(AD)(f)

4. DISCUSSION AND CONCLUSIONS

4.1 Formation of Resonant Seiching Movements

The above model investigations do not at all reproduce exactly the natural configuration of a coast with a detached long shore bar. Indeed the boundary conditions of the wave tank (with a movable flap on the one end and a steep slope on the other) differ very much from those boundaries formed by a submerged structured ridge, a gentle beach slope and the trough in between. Because, however, influences of breaking and broken waves had been excluded sufficiently from the kinematics of partial reflection and re-reflection, in both cases the ADE could be recognized as the accompanying effect of the resonance phenomenon. Extreme water level deflections due to the resonance phenomenon will be formed simply by superimposition of neighboring frequency components. As demonstrated above the requirements of superimposition in the present case are met in such a way, that neighboring frequency components dispose of nearly equal lengths and nearly equal phase angles in the "resonance-frequency range".
The mechanism of resonance with respect to the boundaries at a ridge coast can be described as follows:
Because of the geometry of the trough between beach and bar, boundary conditions for different modes of forced seiching movements of a water body are given. The formation of such modes is governed by the necessity that whole-numbered multiples of half-wave lengths comply with the distance between beach and ridge structure. Contrary to Fig.07, however, it is clear that - due to the limited water depth, inclined slopes and friction effects - *partial Clapotis* waves can develop only, see Fig.05. Hence, in total there is an *ensemble* of proper harmonic modes each assigned by partial clapotis envelopes.
Adequately the overall kinematics can be described as an *ensemble of resonators* (each disposing of a single natural frequency). Different resonances appearing at the same time in this case can be allotted to the resonators absorbing the energy densities from proper frequency components of the wave spectrum traversing the ridge.
In principle such proper kinematics and corresponding envelopes can be formed by sub-frequency ranges Δf_i whose neighboring frequency components tend to adapt their wave lengths to the existing boundaries. Hence, the components of such sub-frequency ranges Δf_i can be named "adapted frequencies" appropriately.
Starting from a marked frequency component f_{mi} (within the sub-frequency range Δf_i) whose length complies with the boundaries perfectly, neighboring frequency components $f < f_{mi}$ appear upset whereas components $f > f_{mi}$ are elongated.
Because in the total frequency range there are several such marked frequency components (higher harmonic frequencies) f_{mi+1}, f_{mi+2} , f_{mi+3} ..., also in their neighborhoods (within sub-frequency ranges Δf_{i+1}, Δf_{i+2}, Δf_{i+3}…) adaptation of component lengths occurs and by this reason marked jumps must appear in the function L(f).
The pronunciation of different proper envelopes coincidentally, of course, is due to the distribution of the total energy within the spectrum.
In detail the properties of the functions L(f) are marked as follows:

A. With Respect to the Trend in the Total Frequency Range $0 \leq f \leq 0.4$ Hz

The gradient dL(AD)/df > dL(ND)/df, i.e., the wave lengths L(AD) increase significantly less with the frequency decreasing ($f \rightarrow 0$), than L(ND) do, aiming at infinite wave lengths.
Globally, however, also with L(AD) the trend exists that lower frequencies correspond to longer waves. Hence, by contrast to the dispersion dc/df there is no change with respect to the sign of dL/df.

B. With Respect to the Frequency Range Disposing of Remarkable Coherence Values

Due to the distinct changes of dc/df in the frequency ranges assigned by bigger energy densities there are varying gradients dL(AD)/df as well. Actually the deviations cause a wavy or stepped structure of function L(AD)(f).
In particular there are confined sub-frequency ranges of gradients tending to $dL(AD)/df \approx 0$. Such portions do correspond to distinct oscillations in the functions c(AD)(f), conf. also appendices 1a and 2a.

4.2 Effects of the Ridge

The formation and the stability of detached coast parallel sand ridges presumably had been estimated exclusively as beneficial with respect to the protection of beaches located behind them. Actually the

longest wave components of the spectrum are reflected from the seaward slope of the bar and by this reason such energy densities hardly can be found in the spectra of breaking waves in the surf zone BÜSCHING (1976, 1978).
Accordingly at Sylt island FÜHRBÖTER (1974) exclusively pointed at the dissipative character of the ridge. His measurements had been analyzed with respect to transmission coefficients $H_t/H_i = H_2/H_1$ referring to a rather big number of synchronous records at gage locations seaward (S1; 940m) and landward (S2; 225m) of the ridge to be seen from Fig.10. No differentiations had been considered with respect to wind conditions, water levels and wave periods. Most surprisingly, however, FÜHRBÖTER did not mention that there also were transmission coefficients $H_2/H_1 > 1$ indicating a resonance phenomenon.
Contrary WANG and YANG (1976) studied spectral transformation at the same site on Sylt island, differentiating the influences of wind directions, tide water levels and wave intensities. Maximum energy densities and wind velocities were limited, however, to 0.35 m^2/Hz and 9m/s respectively. Considering the effect of the long shore bar their results are as follows:
At winds directed landward dissipation is dominant at low water levels only. At water levels higher than NN+ 0.5m, however, at two out of three measurements the peak energy densities in the trough (station S2) are bigger than at the seaward location S1, conf. Fig.10.
Moreover there is one measurement at wind action directed seaward showing a similar effect. Hence the authors speak about the offshore bar to act as an energy trapper occasionally, but they do not believe that this condition may pose a serious condition to shore erosion but the energy piling up on the shoreward side of the bar might be just sufficient to maintain the permanence of the bar.
As a conclusion, however, it can be stated that indeed there are indications for resonance to be found also in the work of other researchers.
The reason why resonance has not yet been appreciated so far to be one of the most important causes of coastal recessions, can be seen in the fact that storm surge conditions have not yet been posed a problem with respect to such ridge coasts.
Concerning the work on near shore dispersion, only SPERANSKI´s investigations, see KUZNETSOV, S.Y. and SPERANSKI, N. (1990) also refer to a coastal formation of a detached long shore bar.
Hence, his very same measurements show an intensity of the ADE accompanying the resonance of the order, which is known from the author's investigations, see BÜSCHING, F. and SPERANSKI, N. (1996).
Contrary - as demonstrated in the later publication - the investigations by THORNTON and GUZA (1982) and by ELGAR and GUZA (1985), do not clearly support the existence of an ADE.
In view of the fact that erosions of more than 30m extending in the coast perpendicular direction did happen due to storm surge actions rather often at the west coast of Sylt island, evidently resonances can form a plausible explanation of this kind of damages.
Consequently the trough between ridge and beach can be named a distinguished local spot of resonance, in which there is needed very few additional power only to support extreme oscillating movements at its boundaries. Moreover such erosive movements will even be amplified, whenever there are several proper oscillations superimposing coincidentally, confer Fig.14.
In general it has to be pointed out that the kinematics of a *local* spot of resonance must differ essentially from the wave motion at a sloping coastal area without any ridge structures. Hence, theoretical estimations cannot deliver satisfying results in this case. Besides the ADE in particular it can be explained, why wave length of investigations by FÜHRBÖTER (1974) and by BÜSCHING (1978), based on zero crossing evaluation techniques, rather correlate with the dominating wave lengths L_P(AD) of the transformed line spectra but not with the wave lengths L_P(ND), associated with the energy maxima of the frequency spectra presuming the validity of normal dispersion relation. Actually it is $L_{P(AD)} << L_{P(ND)}$.
Equally the discrepancy between spectral peak period T_P[s] and significant wave period $T_{Z,1/3}$[s] (of zero crossing method) has to be mentioned here, which was pointed out by the author already in 1974. Using the former evaluations with respect to the measurements Nr. 3, 4, 9, 10 and 11, the spectra transformed to the lengths axis (Fig.15 and appendices 1a and 2a) can be contrasted by a relation $T_P > T_{Z,1/3}$.
Without differentiating between stations 85m and 100m and supposing a linear relationship

$$T_P = \gamma \cdot T_{Z,1/3} \qquad (06)$$

respective proportional factors are in the range of $1.27 \le \gamma \le 2.58$.

5. SUMMARY OF MAIN FINDINGS

A. Resonance in a Wave Tank due to Re-reflection

- Different resonant seiching modes existing coincidentally in a wave tank are characterized by the kinematics of partial standing waves (→ partial waves).
- Partial waves are composed of a number of neighboring frequency components marked by approximately equal wave lengths and by this reason dispose of an anomalous dispersion property.
- Different resonant seiching modes can be understood as an ensemble of resonators absorbing energy densities from the input spectrum.

B. Storm Wave Resonance at a Ridge Coast

- Wave lengths spectra L(f), calculated from measured anomalous phase speed spectra c(f), in general show smaller wave lengths at energy containing frequencies and dispose of a wavy or stepped structure.
- Different resonant seiching modes existing coincidentally in the trough between ridge and beach correspond to neighbouring frequency components. They can be arranged in line spectra ED(L) and be allotted to the geometry of the trough.
- Resonance absorption and anomalous dispersion form a combined phenomenon even with reference to water bodies enclosed imperfectly.

6. SOME CONSIDERATIONS ON INFLUENCING SEICHING MOVEMENTS AT A RIDGE COAST

As a consequence of the assumed causes of the above resonance, extreme water level deflections should occur not only at the beach face but also at the landward slope of the long shore bar. Hence, the author urgently suggests to verify this result by executing respective field measurements and/or model investigations.

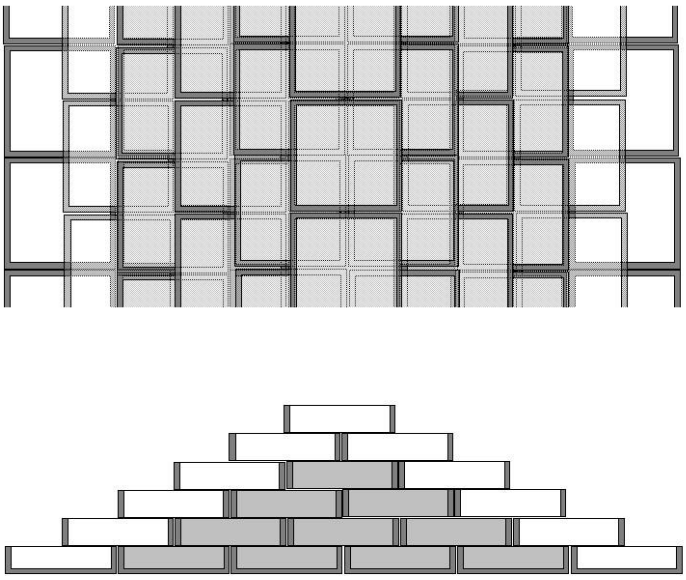

Figure 16: Hollow Element Ridge Crest Structure Composed from Concrete Frames
Upper Part: Top View on Crest Section
Lower Part: Cross Section of Crest Structure

In case such movements are really found to dominate the remaining flow effects, resonance generally can be regarded to be most important with respect to the process of the formation and the stability of sand ridges in front of beaches.

Since maximum Clapotis energies coincide with the maximum water level deflections at the boundaries of the respective water body, taking suitable action on damping of the movements at the beach and/or at the landward slope of the long shore bar can be expected to be most effective.
Because rigid concrete structures cannot be accepted at a recreational beach face, artificial nourishment works commonly are executed instead, however often ineffectively especially as such works need be repeated continually.
Contrary applying protecting structures on top of the ridge, such structures could be made more effectively by hollow concrete elements,- for instance by such concrete frames to be seen from Fig.16. The concrete elements would even be nearly invisible, if their crests do not extend much above SWL.
As was reported earlier, reflection from sloping structures can be influenced extraordinarily by one or two layers of hollow block structures, placed on a slope face regularly. Especially big size hollow elements had been found to be most effective, because the destructive energy at the structure toe is dissipated by some 75 % , see BÜSCHING (1999, 2001). At the configuration, shown in Fig.16, waves coming from sea preferably are dissipated by the seaward slope of the crest structure, whereas still persisting seiching movements in the trough between beach and bar will be reduced by the structured landward slope of the crest structure.
As a consequence, depending on the actual structure height, wave action at the beach face might be reduced by such an extent that no additional beach nourishment is required.

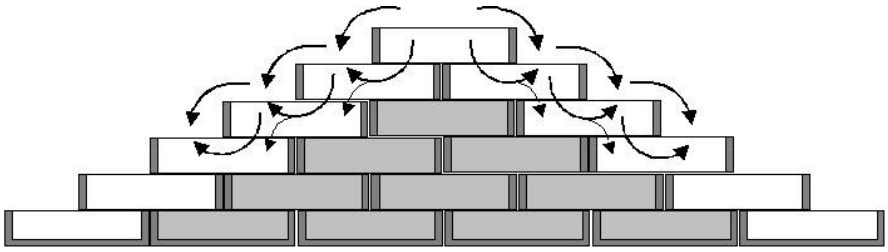

Figure 17: Rough Turbulent Outflow from the Hollow Crest Structure

At the actual structure rough turbulent influx and efflux occur with the waves passing the structure. In Fig.17 the energy consuming vortex conditions due to a lowering wave water level is sketched, whereas opposite vortex directions will occur at the inflow into the structure.
Besides the purpose of dissipating much of the destructive energy of the waves, the respective crest structure disposes of additional advantages:

- Simple design, who's height can be adjusted easily without affecting the dissipation principles
- Considerable air entrainment improves water quality
- Porosity provides protective space for small animals.

As to the Execution of the Crest Structure:

In order to prevent the structure (frames) from being drowned into the sand, an appropriate mat can be placed beneath the bottom frames and/or box structures can be used as a bottom layer, see Fig.17.
The following procedure can be adopted to find out the optimum crest location and structure height:

- Find stable portion of the sand ridge. Column foundation can be applied if necessary.
- Execution of a crest structure disposing of a minimum height at a water level below NSL.
- Monitoring the structure site and measuring waves at stations in the trough and on the beach during storm surge action.
- Improving crest structure where appropriate (for instance in using interlocking elements, increasing dead weight etc.).
- Completing crest structure / increasing structure height by additional frames if necessary.

7. APPENDICES

Appendices 01a and 02a: Frequency spectra of measurements Nr. 04, and Nr. 10 respectively at high tide water levels.
Appendices 01b and 02b: Corresponding spectra transformed to the wave lengths axis.

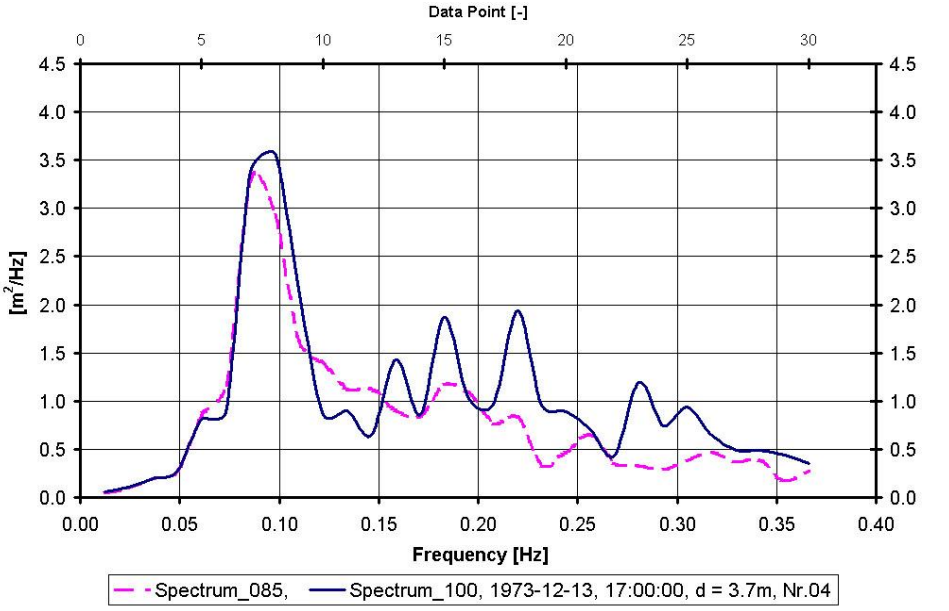

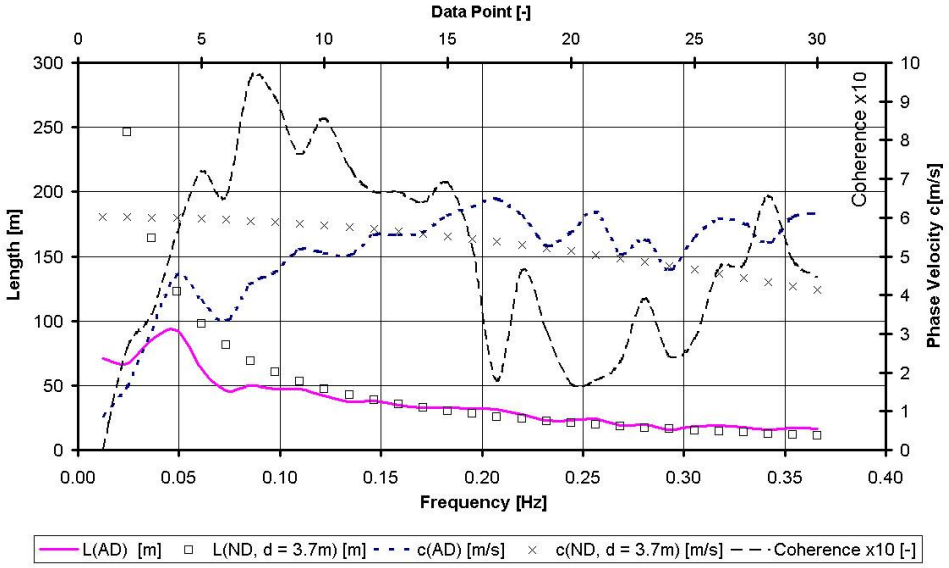

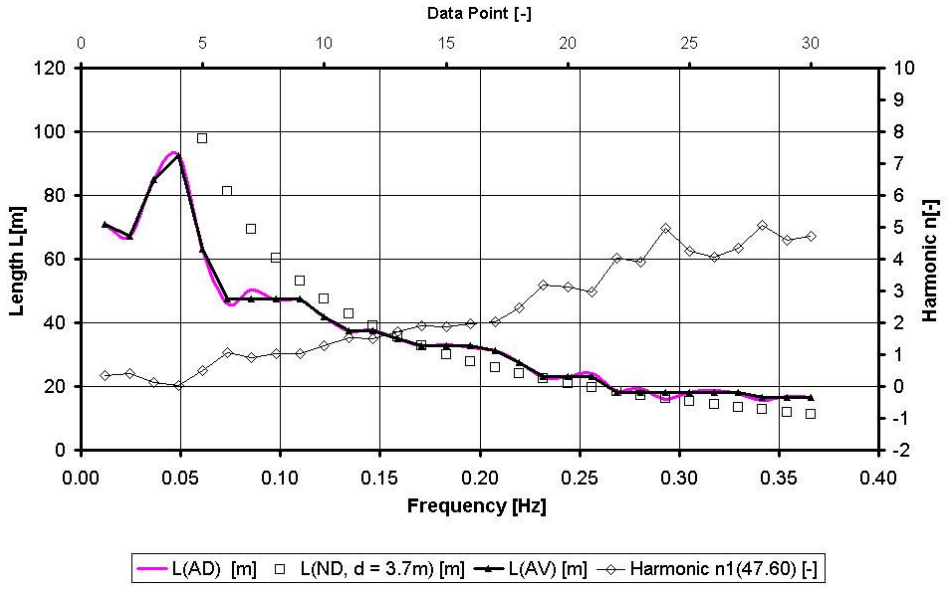

Appendix 01a: Frequency Spectra of Measurement Nr. 04

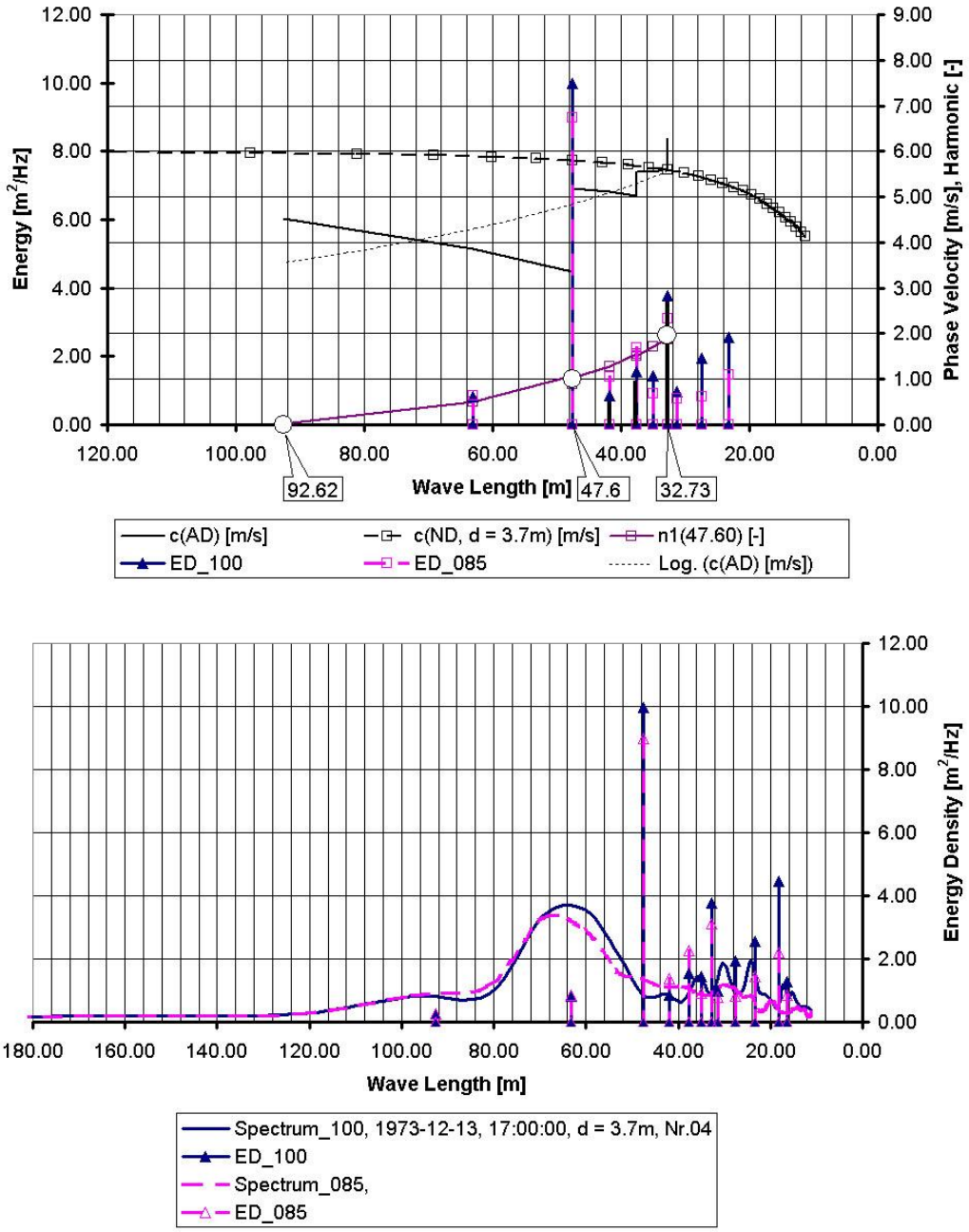

Appendix 01b: Spectra of Measurement Nr. 04 Transformed to the Length Axis

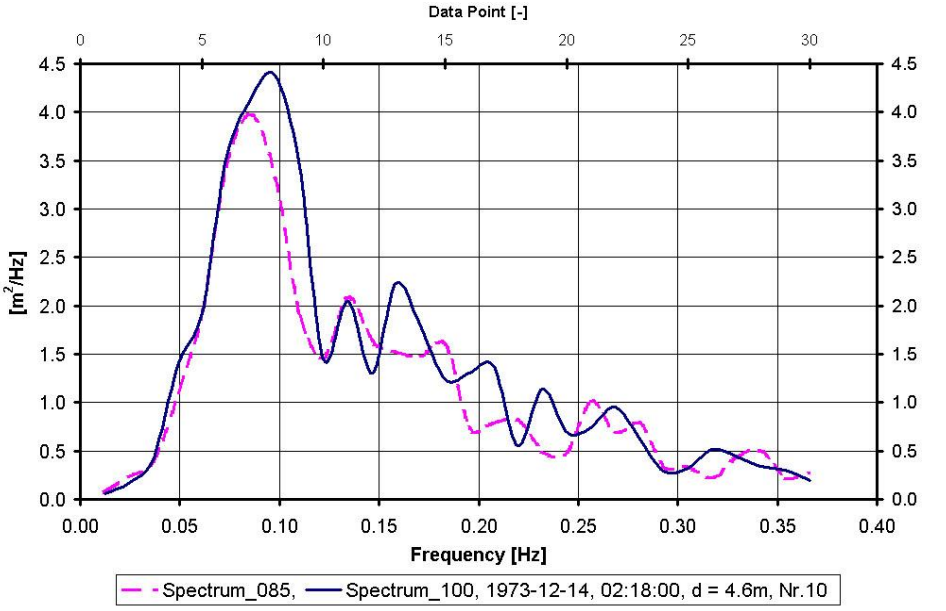

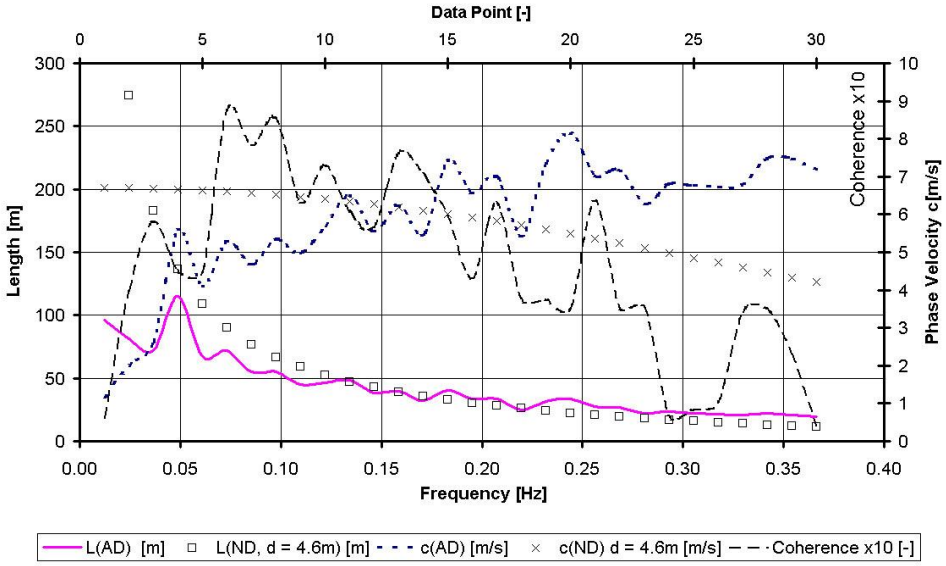

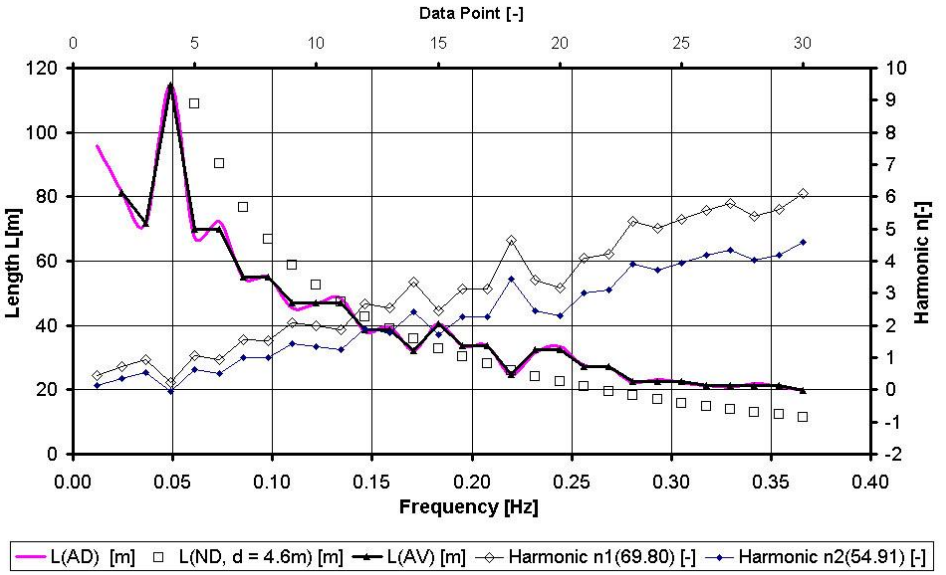

Appendix 02a: Frequency Spectra of Measurement Nr. 10

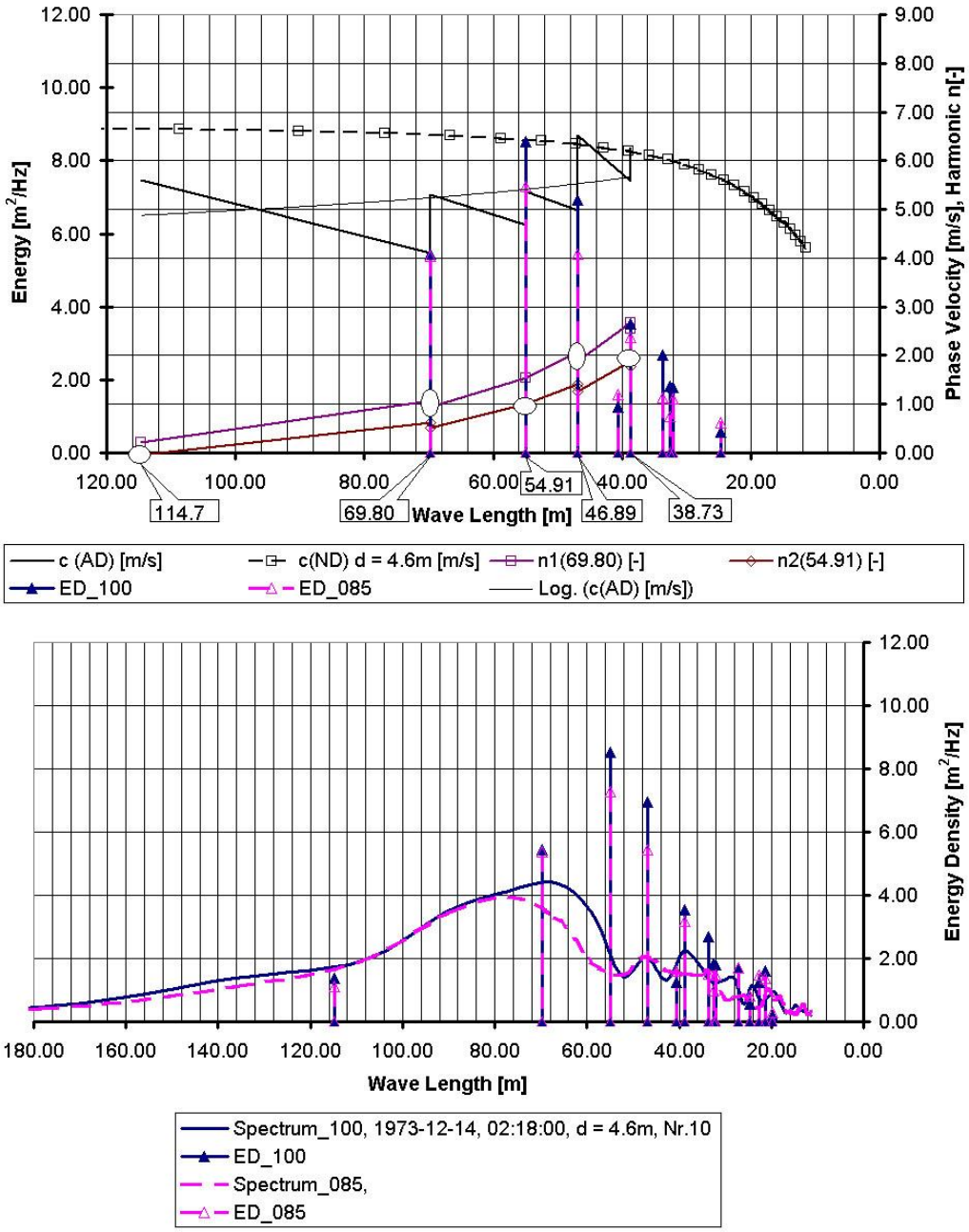

Appendix 02b: Spectra of Measurement Nr. 10 Transformed to the Length Axis

8. REFERENCES

BLEES, O., STÜHMEYER, M. (1991): Wellen und Strömungen vor geböschten Uferschutzbauwerken, Diplomarbeiten Bielefeld University of Applied Sciences, unpublished

BÜSCHING, F. (1974): Über Orbitalgeschwindigkeiten irregulärer Brandungswellen, Mitt. des Leichtweiß-Instituts, TU Braunschweig, H.42, pp.1-256

BÜSCHING, F. (1975): Über die Änderung von Wellenperioden im Brandungsbereich, Mitt. des Leichtweiß-Instituts, TU Braunschweig, H.47, pp. 122-164

BÜSCHING, F (1976).: On Energy Spectra of irregular Surf Waves, Proceedings, 15th Internat. Conference On Coastal Eng., Honolulu, Hawaii, USA, pp. 539-559

BÜSCHING, F. (1978): Wave Deformation due to Decreasing Water Depth, Mitt. des Leichtweiß-Instituts, TU Braunschweig, H.63, pp.167-217

BÜSCHING, F. (1978): Anomalous Dispersion of Surface Gravity Waves in the Near Shore Zone, Proceedings 16th International Conference on Coastal Eng., Hamburg, pp. 21 pages

BÜSCHING, F. (1979): Anomale Dispersion zur Darstellung der küstennahen Wellenverformung, Die Küste H.34, Westholsteinische Verlagsanstalt Boyens u. Co., Heide, pp. 159-183
BÜSCHING, F. (1980): Neue Aspekte bei der Beurteilung küstennaher Wellentransformation und Energieumwandlung, 8. Aufbauseminar MEERESTECHNIK, TU Berlin, pp. D1-D22
BÜSCHING, F. (1980): Doppler Aspects of Near-Shore Wave Transformation, EUROMECH 114, Wladyslawowo, Poland, pp.1-6
BÜSCHING, F. (1982): Analogous Dispersion Properties of Surf Zone and Electromagnetic Waves, Proceedings, 18th International Conference on Coastal Eng., Capetown, South Africa, pp.154-171
BÜSCHING, F. (1983): Resonance Absorption Phenomena of Surf Zone Wave Kinematics, 1). Proceedings, 20th I.A.H.R.-Congress, Vol.VII, Moscow, USSR, pp. 141-145, 2). Proceedings, OCEAN ENGINEERING VII, Taipei, Republic China, 12 pages
BÜSCHING, F. (1986): Wave Transformation and Dispersion with special Reference to the Post Breaking Zone, 1st Internat. Symposium on Harbours, Port Cities and Coastal Topography, Haifa, Israel, pp.39-42
BÜSCHING, F. (1991): Durchströmbare Böschungsstrukturen, Bauingenieur 66, pp. 11-14
BÜSCHING, F. (1991): Embankment Protection Structure; European Patent Office Nr. 91103801.6-2303, pp. 1-47, Versions: English, German, French, Dutch.
BÜSCHING, F. (1992): Wave and Downrush Interaction on Sloping Structures, Proc. 10th International Harbour Congress, Antwerpen, pp. 5.17-5.25
BÜSCHING, F. (1994): Imperfect Reflection from permeable Revetment Structures, 1st International Colloquium CAE TECHNIQUES, Rzeszow, Poland, pp.177-189
BÜSCHING, F. (1995): Hollow Revetment Elements, Proc. COPEDEC IV, Rio de Janeiro, pp.961-976, Brazil
BÜSCHING, F. (1999): Reflection from Hollow Armour Units, Proc. COPEDEC V, Cape Town, pp.1362-1370, South Africa
BÜSCHING, F.(1999): „Reflection Estimates Derived from Structural Response Spectra",4th Int. Colloquium Cax Techniques, Bielefeld, pp. 401-410
BÜSCHING, F. (2000): Dispersion and Reflection at Sloping Structures, Proc. PDCE´2000 Conference Vol.I, pp.29-38, Varna, Bulgaria
BÜSCHING, F. (2001): Combined Dispersion and Reflection Effects at Sloping Structures, Proc. On Port and Maritime R&D and Technology, Vol.I pp. 411-418, Singapore
BÜSCHING, F. (2001): HOLLOW CUBES – Durchströmbare Hohlformkörper als Bauelemente wellenbelasteter Böschungsabdeckungen - HANSA –International Maritime Journal - C 3503 E, 138, H. 10 pp.62-65
BÜSCHING, F. (2003): Sturmwellenresonanz an der Westküste der Insel Sylt, Die Küste H. 67, in printing
BÜSCHING, F., SPERANSKI, N. (1996): Dispersionseffekte bei Schwerewellen im Flachwasser 1. Die Küste Heft 58, pp. 161-177, 2. Papers on Coastal Engineering (Beiträge aus dem Küsteningenieurwesen), FH Bielefeld, Abt. Minden, Nr. 4, 19 pages, Dispersion Effects of Shallow Water Gravity Waves
BÜSCHING, F. (2001): http://www.hollow-cubes.de
ELGAR, S., GUZA, R.T. (1986): Shoaling gravity waves: comparison between field observations, linear theory and nonlinear model, Fluid Mech. vol. 158, pp.47-70
FÜHRBÖTER, A., BÜSCHING, F. (1974): Wave Measuring Instrumentation for Field Investigations on Breakers, Internat. Symposium On Ocean Wave Measurement and Analysis, New Orleans, USA, pp.649-668
FÜHRBÖTER, A. (1974): Einige Ergebnisse aus Naturuntersuchungen in Brandungszonen, Mitt. des Leichtweiß-Instituts, TU Braunschweig, H.40, S. 331-371
FÜHRBÖTER, A. (1979): Sandbewegung im Küstenraum, Rückschau, Ergebnisse und Ausblick, DFG Forschungsbericht, Harald Boldt Verlag Boppard
HAGEMEYER, K., KRAMER, M. (1992): Reflexion irregulärer Wellen an geböschten Uferschutzbauwerken, Diplomarbeiten Bielefeld University of Applied Sciences, unpublished
KUZNETSOV, S. Y., SPERANSKI, N. (1990): Phase Velocity of Free and Forced Waves in Shallow Water. In: "Modern processes of sedimentation on shelf", pp. 180-186, "Nauka", Moscow, (in Russian)
SPERANSKI, N., BÜSCHING, F. (1996): Dispersion Effects in Shallow Water Gravity Waves; Proc. European Geophysical Society, General Assembly, pp.C685 The Hague, The Netherlands
THORNTON, E., GUZA, R.T. (1982): Energy Saturation and Phase Speed Measured on a Natural Beach, J. Geophys. Res. C86(5): pp. 4149-4160
WANG, H., YANG, W.-C. (1976): Measurements and Computation of Wave Spectral Transformation at Island of Sylt, North Sea, Mitt. d. Leichtweiß – Instituts der Techn. Universität Braunschweig, Heft 52